2D NOVEL STRUCTURES ALONG AN OPTICAL FIBER

CHARLES-JULIEN VANDAMME and STEFAN C. MANCAS†

*Dept. Math & Mechanics ENSEIRB-MATMECA, Institut Polytechnique de Bordeaux
Talence 33402, France*

†*Department of Mathematics, Embry-Riddle Aeronautical University, Daytona-Beach
Florida 32114, USA*

Abstract. Bu using spectral methods, we present seven classes of stable and
unstable structures that occur in a dissipative media. By varying parame-
ters and initial conditions we find ranges of existence of stable structures
(spinning elliptic, pulsating, stationary, organized exploding), and unstable
structures (filament, disorganized exploding, creeping). By varying initial
conditions, vorticity, and parameters of the equation, we find a reacher be-
havior of solutions in the form of creeping-vortex (propellers), spinning rings
and spinning "bean-shape" solitons. Each class differentiates from the other
by distinctive features of their shape and energy evolution, as well as domain
of existence.

1. Introduction

Such as the nonlinear Schrödinger equation (NLSE), the **complex cubic-quintic
Ginzburg-Landau equation** (CCQGLE) is one of the most intensively studied
equation describing weakly nonlinear phenomena in dissipative systems [3]. Thus,
much work has been done about the features and the properties of this equation as
well as its numerous applications such as nonlinear waves, superconductivity, su-
perfluidity [6], Bose-Einstein condensation, Bénard convection [1] and nonlinear
optics [7].
Solitary waves (or solitons) are self localized solutions of certain nonlinear PDEs
describing the evolution of a dissipative system [8]. Whereas traditional solitons
are stationary in time and preserve their shape upon interaction, some dissipative
soliton solutions of the CCQGLE are non stationary. In Hamiltonian systems, sta-
tionary solitons exist as a result of a balance between diffraction/dispersion and

nonlinearity. However, a dissipative system is known to be far from equilibrium and is defined by energy exchanges with external sources. Thus, there is no conserved quantity, which implies that they are not Hamiltonian systems. In dissipative systems, solitons are obtained by balancing gain and loss. As a result, whereas solutions are defined by one parameter family in Hamiltonian systems, in dissipative systems solutions are obtained with varying amplitude and width that are fixed by the parameters of the equation. Therefore, the inverse scattering method [1] which is used to calculate solutions of integrable and some non integrable Hamiltonian systems cannot be used in our case. In this paper, we present new classes of soliton solutions of the CCQGLE and we analyze both their shape and energy evolution that depends strongly on the parameters used, and choice of initial conditions. The development of powerful numerical tools over the last decades lead us to use an accurate spectral method for the spatial discretization, together with a 4th order Adams-Bashforth scheme for temporal discretization. Due to the intensive computations codes in Fortran 90, we run simulations on ZEUS cluster (256 nodes dual Xeon 3.2 GHz processors, 1024 KB cache 4GB with Myrinet) at Embry-Riddle Aeronautical University. For each class of solitons, simulations lasted from several hours to several days.

2. Numerical Scheme of the 2D CCQGLE

Numerical simulations are based on the 2D CCQGLE model (1) with **transverse Laplacian** $\nabla_\perp^2$ that takes into account spatial diffraction in the paraxial wave approximation. Quintic terms are essential in order to obtain stable solitons [1]

$$\partial_z A = \epsilon A + (b_1 + \mathrm{i}c_1)\nabla_\perp^2 A - (b_3 - \mathrm{i}c_3)|A|^2 A - (b_5 - \mathrm{i}c_5)|A|^4 A. \quad (1)$$

Here $A(x, y; z)$ is the normalized envelope of the field which is a complex function, x and y are the transverse spatial coordinates and z is the propagation distance along the optical fiber (or cavity depth). The physical parameters of the system are: ϵ linear gain/loss, b_1 angular spectral filtering, $c_1 = 0.5$ second-order diffraction coefficient, b_3 nonlinear gain/loss, $c_3 = 1$ nonlinear dispersion, b_5 saturation of the nonlinear gain/loss, and c_5 saturation of the nonlinear refractive index. The solutions to (1) will be computed using a Fourier spectral method in which we will monitor the energy $Q(z) = \int_{-\infty}^\infty \int_{-\infty}^\infty |A(x, y; z)|^2 \, \mathrm{d}x\mathrm{d}y$. For a localized solution, Q is finite and changes smoothly while the solution stays within the region of existence of the soliton. When Q changes abruptly there is a bifurcation and the solution jumps from a branch of solitons that become unstable to another branch of stable solitons, or vice versa. As soon as the solution becomes unstable, Q diverges until infinity or collapses to 0. For a certain class of solutions, Q will evolve periodically in some regime, and will converge to a finite value [10].

Table 1. Initial sets of parameters for 2D solitons.

2D solitons	ϵ	b_1	c_1	b_3	c_3	b_5	c_5
elliptic spinning and filament	-0.1	0.1	0.5	-0.8	1	0.04	-0.02
pulsating and stationary	-0.045	0.04	0.5	0.37	1	0.05	-0.08
exploding	-0.1	0.125	0.5	-1	1	0.1	-0.6
creeping and propeller	-0.1	0.101	0.5	-1.3	1	0.3	-0.101

3. Parameters and Initial Conditions

The main goal of this study is to find continuous parameter ranges around a fixed set in which each class of solitons remains stable.

3.1. Parameters

First, an initial set of parameters published in [4] is used for the elliptic, filament, pulsating and exploding classes, while for creeping we use parameters published in [2], see Table 1. Starting from these values, for each class we vary one parameter in a range of width 0.2 while keeping all the other parameters constant. When we are outside of the range of existence of the solitons, we return to the initial value, and vary the other remaining parameters one by one. After several simulations, we noticed that b_3 and ϵ seemed to be the more sensitive, i.e., small changes of b_3 or ϵ implied significant changes of the solution. Thus, a step of 0.01 has been chosen for these parameters whereas a step of 0.05 has been used for b_1, b_5 and c_5. However, this behavior is not a general rule, so, in some cases, a smaller step has been used for the last three parameters.

3.2. Initial and Boundary Conditions

We use two different types of initial conditions, a Gaussian shape $A(x, y; 0) = A_0 \mathrm{e}^{-r^2}$, and a ring shaped vortex $A(x, y; 0) = A_0 r^m \mathrm{e}^{-r^2} \mathrm{e}^{\mathrm{i}m\theta}$ with a vorticity m. A_0 is a real amplitude of the initial condition, and $\theta = \tan^{-1}\left(\frac{\sigma_y y}{\sigma_x x}\right)$ is the phase. The inverse widths (shape) of each of the initial conditions are controlled by the parameters σ_x and σ_y, with $r = \sqrt{(\sigma_x x)^2 + (\sigma_y y)^2}$, see Fig. 1. Since we used a Fourier spectral method, the boundary conditions are periodic and are incorporated in the method. We made sure that the solutions did not reach the boundaries while they evolved, otherwise additional reflection would occur, so we increased the domain to avoid reflective waves.
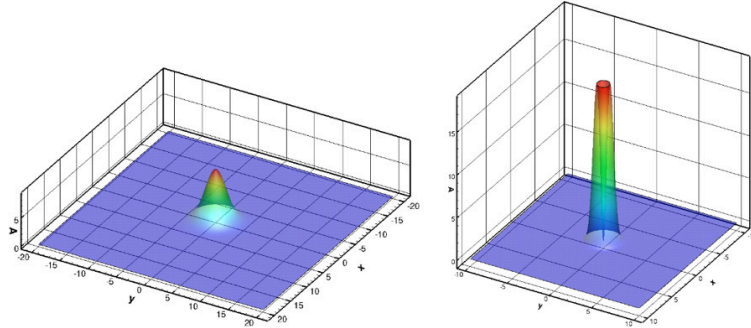
Figure 1. Initial condition. Left: Gaussian shape. Right: ring vortex with vorticity $m = 1$.

4. Simulation Results

4.1. Elliptic Spinning and Filament Solitons

4.1.1. Description

For both of these solutions, the same set of parameters is used, see Table 1, line 1. The difference between them is the type of initial condition, elliptic or circular. For the elliptic vortex, an elliptic Gaussian pulse with widths $\sigma_x = 0.15$, and $\sigma_y = 0.85$. This soliton which lacks radial symmetry has two peaks of amplitude diametrically opposed [4]. The energy first oscillates before converging to a fixed value and remains stationary, see Fig. 2. Increasing the amplitude and choosing the
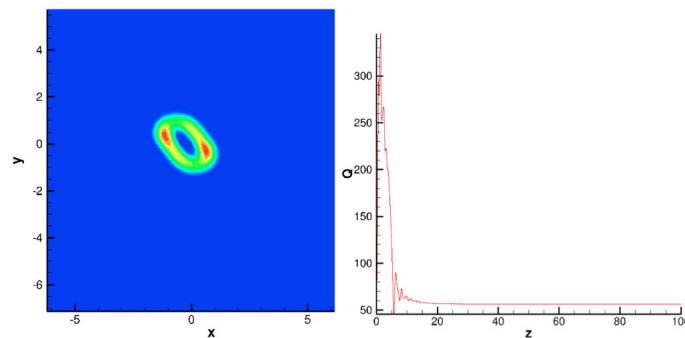
Figure 2. Elliptic spinning soliton. Left: contour plot of the amplitude. Right: energy evolution.

initial condition to be circular, $A_0 = 3.0$, $\sigma_x = \sigma_y = 0.15$ results in a splitting of the initial beam in several bell-shaped solitons which are non spinning. As it has been shown in [4], this class may be unstable and leads to chaos, but for some set

of parameters, the beams stop splitting and the soliton appears to be stable. This result is also observed with higher vorticity. For example, for $m = 2$ see Fig. 3.
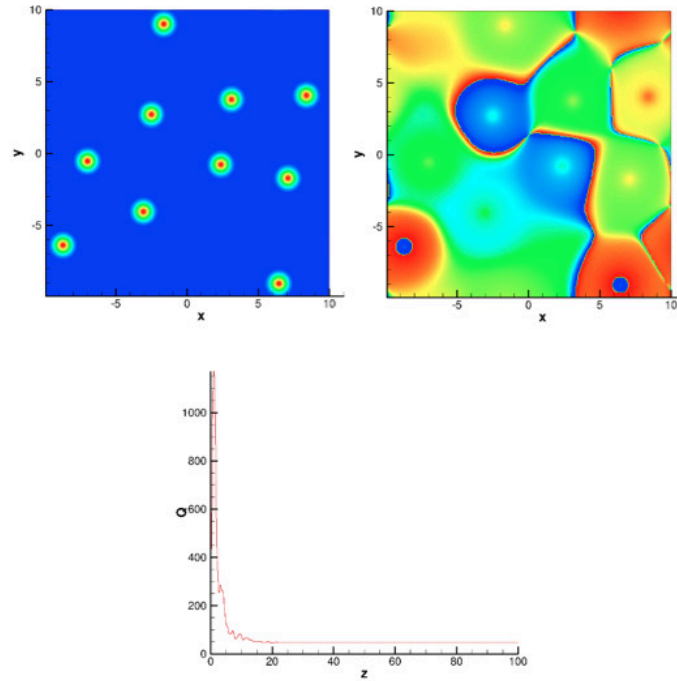

Figure 3. Filament soliton for $m = 2$, $b_5 = 0.180$ that splits in several bell-shape beams and non spinning phase. Top left: contour plot of amplitude. Top right: phase plot. Bottom: energy.

4.1.2. Ranges of Parameters and Bifurcations

Elliptic spinning and filament solitons undergo bifurcations which result in stable solitons over a large parameter range around the initial sets of parameters of Table 1. By varying one parameter in the range from Table 2, several bifurcations happen and other stable solitons appear with an energy evolution similar to these presented in Figs. 2 and 3. The main bifurcations observed lead to the transformation of the initial beam in a stable spinning ring, filament or quite exotic spinning "bean- shape" solitons, see Figs. 4, 5 and 6.

Table 2. Parameter ranges of spinning stable solitons.

Parameters	Initial value	Final value
b_1	0.035	0.235
ϵ	-0.3	-0.1
b_3	-0.9	-0.7
b_5	-0.02	0.18
c_5	-0.22	-0.02
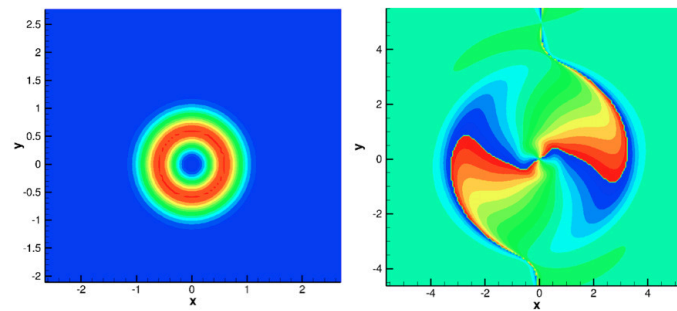
Figure 4. Spinning ring soliton with elliptic vortex initial condition $m = 1$, $b_3 = -0.84$, $z = 50s$. Left: contour plot of amplitude. Right: phase plot that shows spinning.
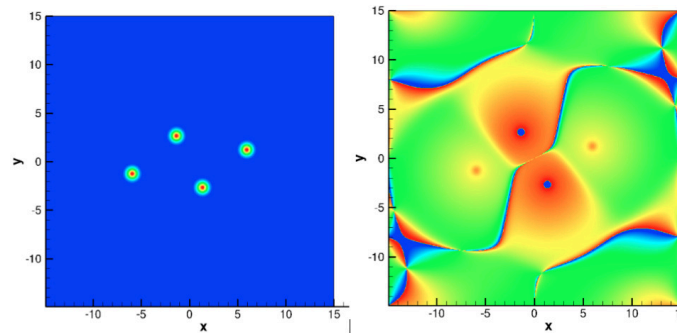
Figure 5. Filament soliton with elliptic vortex initial condition $m = 1$, $b_5 = 0.18$, $z = 100s$. Left: contour plot of amplitude. Right: phase plot that shows no spin.

4.2. Pulsating Solitons

4.2.1. Description

As it was presented in [4], a soliton with a very interesting pulsating behavior was discovered for a slightly asymmetric ($A_0 = 5.0$, $\sigma_x = 0.8333$, $\sigma_y = 0.9091$)
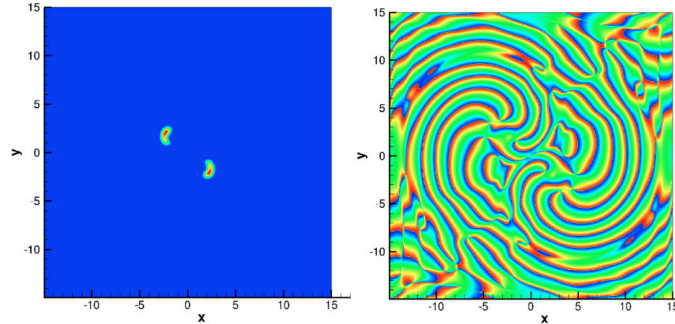
Figure 6. Spinning "bean-shape" soliton with elliptic vortex initial condition $m = 1$, $\epsilon = -0.17$, $z = 50s$. Left: contour plot of amplitude. Right: phase plot.

Gaussian beam. For the set of parameters of Table 1, line 2, the soliton evolves first as a stationary one, but after a certain time, its energy increases and takes a pulsating behavior before increasing again to a new stationary state. During the pulsating period, the soliton keeps a radially symmetric bell shape profile at the maximum of energy, whereas for the minimum value of Q, the beam elongates alternatively in different directions. However, other pulsating solitons exist and do not evolve in the same way. For example, for two values of b_3, the energy evolves differently, see Fig. 7. With $b_3 = 0.37$, after a short pulsating behavior, the soliton reaches a stationary stable state until $z \approx 420s$. Following that a perturbation appears which makes the soliton evolve towards a higher state with a new pulsating energy. This pulsating behavior lasts around $100s$. For $b_3 = 0.40$, the first stationary state does not appear, the energy seems to be collapsing before reaching the pulsating state very fast. This pulsating state lasts in this case for almost $200s$. Furthermore, the energy values that both solitons reach after the pulsating state are relatively different ($Q \approx 60$ for $b_3 = 0.37$ and $Q \approx 100$ for $b_3 = 0.40$). However, despite the differences observed relating to the evolution of the energy, for $b_3 = 0.40$ the structure has the same dynamic behavior as described above during the pulsating state, see Fig. 8.

4.2.2. Ranges of Parameters and Bifurcations

In the ranges of parameters explored, the pulsating soliton experiences a bifurcation that leads to a stationary bell shaped soliton, see Fig. 9. The parameter b_5 seems to be a very sensitive parameter for the pulsating soliton. Indeed, whereas for $b_5 \in [-0.05; -0.02]$ the soliton is pulsating, from 0.06 to 0.18 solitons are stationary and from -0.02 to 0.04 solitons are unstable. Outside of these ranges, from -0.02 until 0.04, solitons are unstable. Table 3 gives an overview of the parameter ranges explored for the pulsating and stationary solitons.
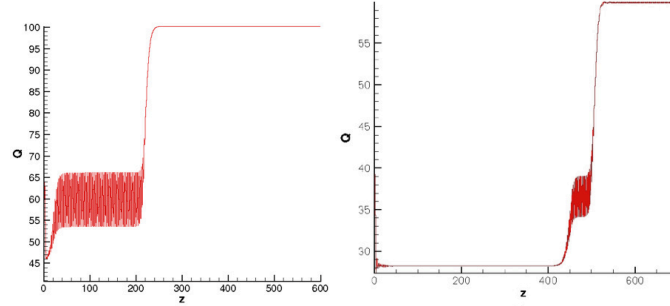
Figure 7. Energy of pulsating solitons. Left: $b_3 = 0.40$. Right: $b_3 = 0.37$.

Table 3. Parameter ranges of existence of pulsating and stationary solitons.

Parameters	Pulsating	Stationary (non pulsating)
b_1	[0.015; 0.035]	[0.085; 0.235]
ϵ	[-0.095; -0.045]	[-0.245; -0.105]
b_3	[-0.4; -0.36]	[-0.35; -0.20]
b_5	[-0.05; -0.02]	[0.06; 0.18]
c_5	[-0.09; -0.08]	[-0.23; -0.11]

4.3. Exploding Solitons

4.3.1. Description

For this class we use a radially symmetric Gaussian beam with amplitude $A_0 = 3$, $\sigma_x = \sigma_y = 0.3$, and parameters from line 3 of Table 1. The main feature of this soliton is that it explodes intermittently and periodically resulting in significant bursts of energy, while after each explosion, the soliton recovers its initial shape, see Fig. 10. The evolution starts from a stable bell shaped structure. Then, circular waves appear around the the initial beam developing from center to the exterior. Suddenly and violently, the soliton explodes, it grows up fast keeping radial symmetry, and recovers its initial shape after an explosive phase. Even if the soliton always returns to the same shape, the explosions are not strictly identical as we can see in Fig. 10. The evolution of the structure during a full explosion process is shown in Fig. 11.

4.3.2. Ranges of Parameters and Bifurcations

Outside of the ranges of existence of exploding soliton from Table 4, we found two types of solitons. The stable stationary solitons, and unstable ones for which
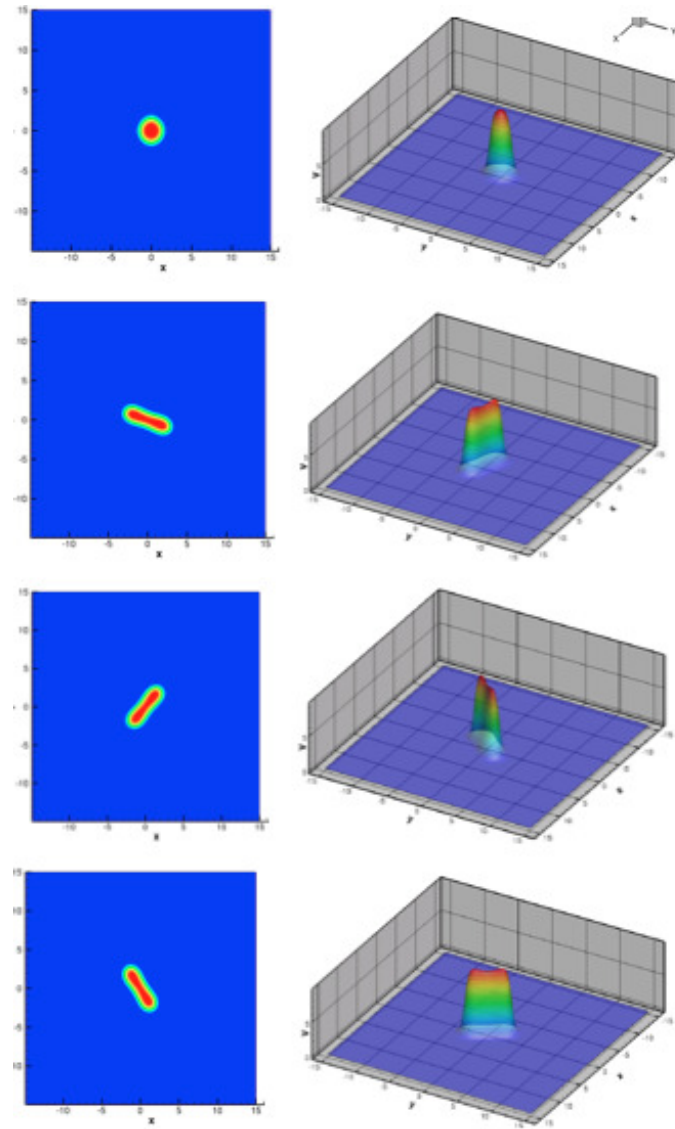
Figure 8. Shape evolution and elongation during the pulsating state for $b_3 = 0.40$. From top to bottom, $z = 90s, z = 120s, z = 135s, z = 150s$.

the energy diverges to infinity. The later type never recovers their shape, and appears probably when the features of the system and the medium (defined by the parameters of the CCQGLE) cannot compensate the energy bursts, and hence let the energy grow without bound.
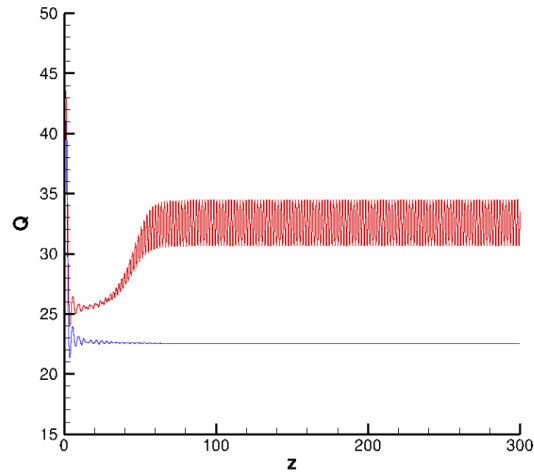
Figure 9. Bifurcations for pulsating soliton for $b_3 = -0.36$ (top energy in red) that becomes stationary bell shaped soliton for $b_3 = -0.35$ (bottom energy in blue).
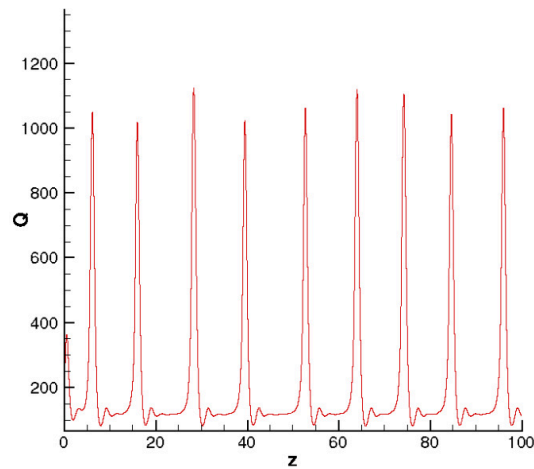

Figure 10. Exploding soliton: evolution of the energy which shows periodic bursts and recovery.

As it was explained previously, small changes in some parameters dramatically change features of the exploding soliton. As it is shown in Fig. 12, the effect of changing b_3 shows an energy evolution with random amplitudes and shifts. Also, depending on the initial conditions, the explosions may be organized or disorganized, as we can see in Fig. 13.
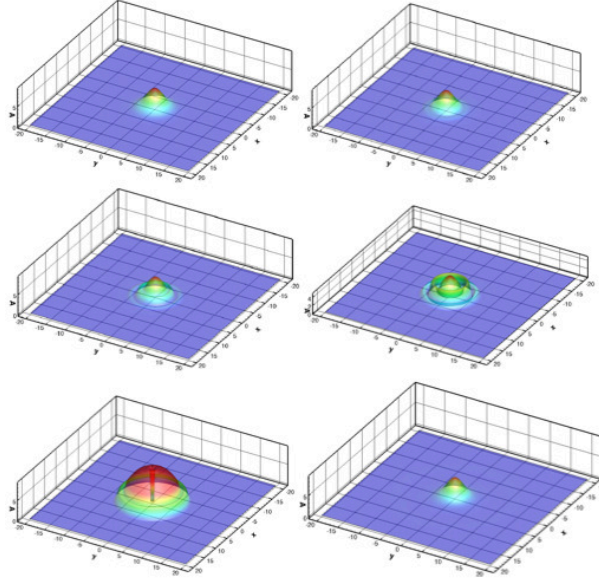
Figure 11. Explosion process corresponding to Fig. 10. From top to bottom row wise, $z = 10s$, $z = 12s$, $z = 14s$, $z = 15s$, $z = 16s$, $z = 18s$.

Table 4. Parameter ranges of existence for organized exploding solitons.

Parameters	Range
b_1	[0.135; 0.235]
ϵ	[-0.3; -0.1]
b_3	[-1.0; 0.8]
b_5	[0.09; 0.15]
c_5	[-0.6; -0.4]

A ring vortex initial condition has been tested in the same ranges of parameters. Contrary to pulsating solitons which did not exist with this initial shape, exploding solitons seemed to be existing. However, even when explosions and bursts happened, the behavior of such a soliton was extremely unpredictable. In fact, the evolution of the energy is very random, explosions do not appear periodically and the amplitudes of these explosions are relatively different, see Fig. 13. We assume that this initial condition leads to an exploding soliton that is on transition to chaos.
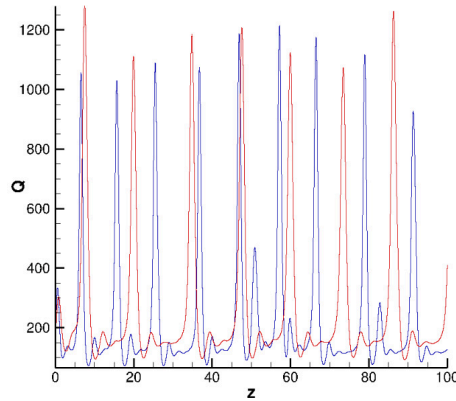
Figure 12. Energies of two exploding solitons obtained with $b_3 = -0.96$ (blue) and $b_3 = -0.81$ (red): the explosions are shifted with different bursts.

Table 5. Parameter ranges of existence for disorganized exploding solitons

Parameters	Range
b_1	[0.085; 0.135]
ϵ	[-0.26; -0.1]
b_3	[-1.0; 0.8]
b_5	[0.13; 0.15]
c_5	[-0.6; -0.5]

4.4. Creeping Solitons

4.4.1. Description

Creeping soliton dynamic behavior also starts from a Gaussian initial condition with radial symmetry, with $A_0 = 3.0$ and $\sigma_x = \sigma_y = 0.3$. In 2D, creeping solitons behave like tumors. In fact, they spread in all directions until filling the domain. Thus, the energy of a 2D creeping soliton is very often characterized by a constant raise, hence precautions must be taken when the size of the domain is defined. Before spreading and filling the numerical grid, creeping solitons present a very complex dynamic evolution pattern by taking surprising geometrical shapes that resemble fractals. They are still chaotical while but localized in the domain and tend to show some symmetry. In the 1D case, it has been proved [5] that the region of parameters where creeping solitons exist is filled which a rich variety of bifurcations between, stationary, pulsating and creeping solitons.
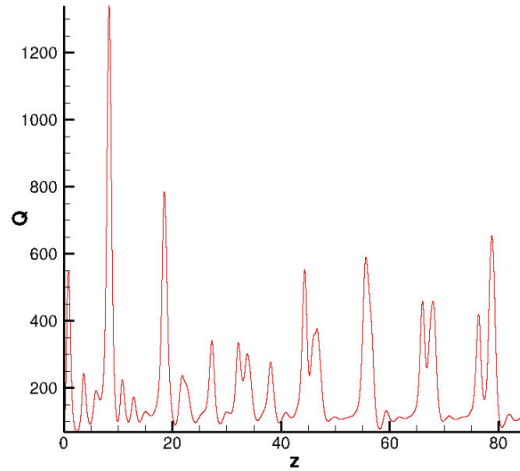
Figure 13. Disorganized exploding soliton starting as a ring vortex with $m = 1$, and $b_5 = 0.14$

.

4.4.2. Ranges of parameters

Two main bifurcations were observed by varying parameters of Table 1, line 4. The first one takes the shape of a ring which is expanding very fast and leads to chaos, the second one leads to stationary solitons. The parameters ranges are presented in Table 6.

Table 6. Parameter ranges of existence. Left: creeping solitons. Right: stationary solitons.

Parameters	Range creeping	Range stationary
b_1	[0.08; 0.14]	not found
ϵ	[-0.13; -0.09]	[-0.3; -0.14]
b_3	[-1.3; -1.29]	[-1.28; -1.11]
b_5	[0.3; 0.31]	[0.32; 0.36]
c_5	[-0.101; -0.100]	[-0.8; -0.6]

By changing the initial condition into a ring vortex of vorticity $m = 1$, a novel class, spreading vortex soliton has been found. This soliton has exactly the same behavior as the creeping, but it is also spinning and that creates interesting "propeller" shapes before spreading and filling the domain, see Fig. 15. The energy of such structure starts oscillating (during this phase the beam alternatively grows up and comes back to its initial shape) and finally converges to a fixed value that takes the shape of a ring vortex. Fig. 16 shows the evolution of the energy of a propeller
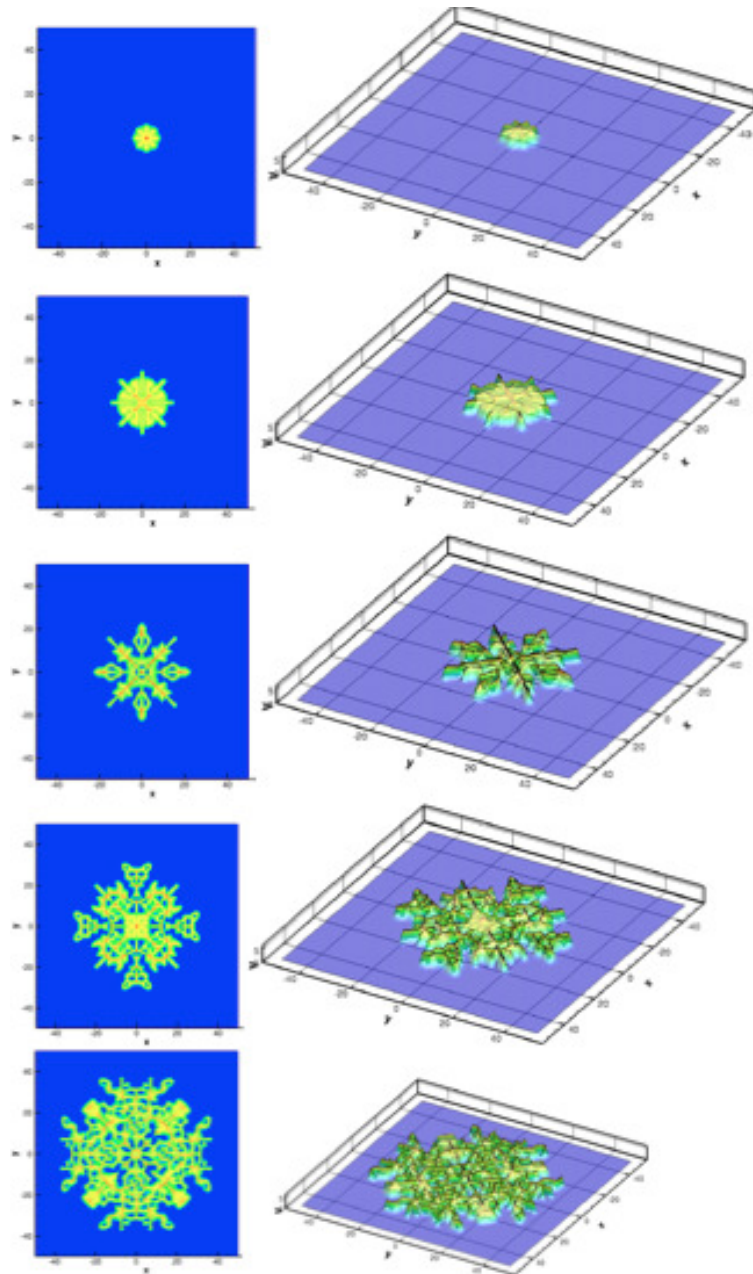
Figure 14. 2D Creeping soliton: Gaussian beam is spreading like a fractal.

soliton emphasizing this bifurcation: the energy oscillates and seems to start converging but then a perturbation makes the energy diverge and increase because of

the spreading behavior of the solution. Table 7 shows a comparison between the propeller and the ring spinning type. If one compares the energy between the two, it seems like a battle between the increasing behavior of the creeping together with the spinning behavior of the ring, when the energy wants to remain bounded.
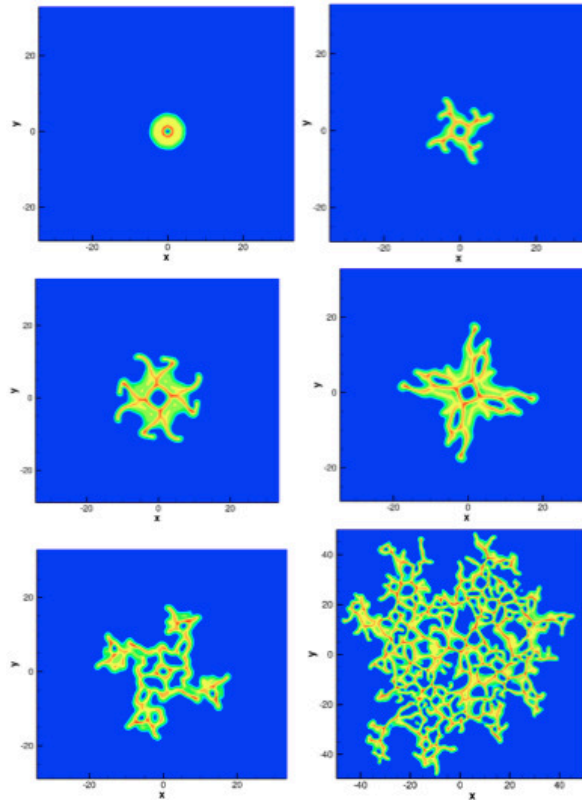

Figure 15. Evolution of the shape of a propeller soliton.

Table 7. Parameter ranges. Left: spreading spinning solitons. Right: ring spinning solitons.

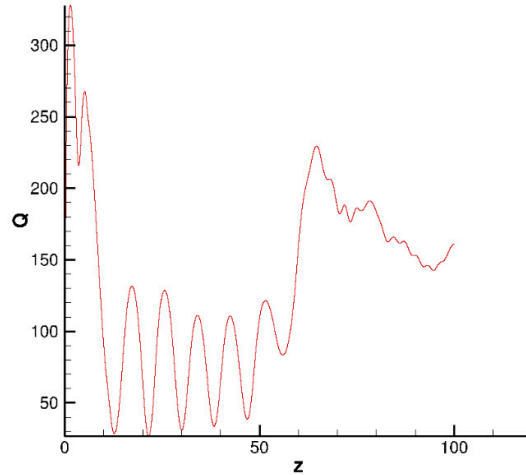| Parameters	Range propeller	Range ring spinning
b_1	[0.08; 0.14]	[0.185; 0.235]
ϵ	[-0.19; -0.09]	[-0.3; 0.2]
b_3	[-1.3; -1.23]	[-1.22; -1.11]
b_5	[0.3; 0.36]	not found
c_5	[-0.1; -0.06]	not found

Figure 16. Evolution of the energy of a spreading spinning soliton next to the bifurcation boundary.

Conclusion

In conclusion, we have found fascinating (2+1)D structures in dissipative media predicted by the complex cubic-quintic Ginzburg-Landau equation. Different types of solutions, spinning or not, such as elliptic vortex, filament, pulsating, exploding and creeping solitons have been categorized by focusing on their energy, shape and phase evolution. Regions of existence of these types of soliton have also been calculated in the five dimensional parameter space given by the physical parameters of the equation. The study revealed interesting ranges and bifurcations for each structure. Whereas non spinning structures have mainly lead to stable stationary solitons, due to bifurcations spinning structures, symmetric or asymmetric, split and have revealed to be no spin solitons. By changing the initial conditions, and increasing the vorticity, allowed us to observe for the first time new types of solutions such as disorganized exploding and propeller solitons.

References

[1] Ablowitz M. and Clarkson P., *Solitons, Nonlinear Evolution Equations and Inverse Scattering,* London Mathematical Society Lecture Notes Series vol. 149, Cambridge Univ. Press, Cambridge 1991.

[2] Akhmediev N., Soto-Crespo J. and Town G., *Pulsating Solitons, Chaotic Solitons, Period Doubling, and Pulse Coexistence in Mode-Locked Lasers*: *Complex Ginzburg-Landau Equation Approach*, Phys. Rev. E **63** (2001) 56602.

[3] Aranson I. and Kramer L., *The World of The Complex Ginzburg-Landau Equation*, Rev. Mod. Phys. **74** (2002) 99-143.

[4] Bérard F. and Mancas S., *Spatiotemporal Two-Dimensional Solitons in the Complex Ginzburg-Landau Equation*, Advances and Applications in Fluid Mechanics **8** (2010) 141-156.

[5] Chang W., Ankiewicz A. and Akhmediev N., *Creeping Solitons in Dissipative Systems and Their Bifurcations*, Physical Review E **76** (2007) 016607

[6] Fabrizio M., *Ginzburg-Landau Equations and Second Order Phase Transitions*, International Journal of Engineering Science **44** (2006) 529-539.

[7] Malomed B., Gölles M., Uzunov I. and Lederer F., *Stability and Interactions of Pulses in Simplified Ginzburg-Landau Equations*, Phys. Scr. **55** (1997) 73-79

[8] Newell A., *Solitons in Mathematics and Physics*, CBMS-NSF Regional Conference Series in Applied Mathematics, SIAM, Philadelphia 1985.

[9] Press W., Teukolsky S., Vetterling W. and Flannery B., *Numerical Recipes in Fortran 90*, 2nd Edn, Cambridge University Press, Cambridge 1996.

[10] Soto-Crespo J., Akhmediev N., Devine N. and Mejía-Cortés C., *Transformations of Continuously Self-Focusing and Continuously Self-Defocusing Dissipative Solitons*, Optics Express **16** (2008) 15388-15401

[11] Soto-Crespo J., Akhmediev N. and Grelu P., *Dissipative Ring Solitons with Vorticity*, Optics Express **17** (2009) 4236-4250